HHS Public Access

Author manuscript

Sens Actuators B Chem. Author manuscript; available in PMC 2019 February 01.

Published in final edited form as:

Sens Actuators B Chem. 2018 February ; 255(3): 3654–3661. doi:10.1016/j.snb.2017.10.005.

Laminated and infused Parafilm® - paper for paper-based analytical devices

Yong Shin Kim[a], **Yuanyuan Yang**[b], and **Charles S. Henry**[b,c,*]

[a]Department of Applied Chemistry, Hanyang University, Ansan 15588, Republic of Korea

[b]Department of Chemistry, Colorado State University, Fort Collins, Colorado 80523, United States

[c]Department of Biomedical Engineering, Colorado State University, Fort Collins, Colorado 80523, United States

Abstract

Numerous fabrication methods have been reported for microfluidic paper-based analytical devices (μPADs) using barrier materials ranging from photoresist to wax. While these methods have been used with wide success, consistently producing small, high-resolution features using materials and methods that are compatible with solvents and surfactants remains a challenge. Two new methods are presented here for generating μPADs with well-defined, high-resolution structures compatible with solvents and surfactant-containing solutions by partially or fully fusing paper with Parafilm® followed by cutting with a CO_2 laser cutter. Partial fusion leads to laminated paper (*l*-paper) while the complete fusion results in infused paper (*i*-paper). Patterned structures in *l*-paper were fabricated by selective removal of the paper but not the underlying Parafilm® using a benchtop CO_2 laser. Under optimized conditions, a gap as small as 137 ± 22 μm could be generated. Using this approach, a miniaturized paper 384-zone plate, consisting of circular detection elements with a diameter of 1.86 mm, was fabricated in 64 × 43 mm^2 area. Furthermore, these ablation-patterned substrates were confirmed to be compatible with surfactant solutions and common organic solvents (methanol, acetonitrile and dimethylformamide), which has been achieved by very few μPAD patterning techniques. Patterns in *i*-paper were created by completely cutting out zones of the *i*-paper and then fixing pre-cut paper into these openings similar to the strategy of fitting a jigsaw piece into a puzzle. Upon heating, unmodified paper was readily sealed into these openings due to partial reflow of the paraffin into the paper. This unique and simple bonding method was illustrated by two types of 3D μPADs, a push-on valve and a time-gated flow distributor, without adding adhesive layers. The free-standing jigsaw-patterned sheets showed good structural stability and solution compatibility, which provided a facile alternative method for fabricating complicated μPADs.

*Author to whom correspondence should be addressed. chuck.henry@colostate.edu; Tel.: +1 970 491 2852.

Keywords

Microfluidic paper-based analytical device; Parafilm® paper; Paper zone plate; Paper-based valve; Paper-based flow distributor

1. Introduction

Microfluidic paper-based analytical devices (μPADs) have attracted great attention since the work of Martinez et al. because of their ease of use, low cost, broad availability of materials, and overall performance [1–6]. μPADs are also attractive because they spontaneously generate flow via capillary forces caused by porous hydrophilic paper, and their flow pathways are confined to specified regions typically defined by hydrophobic barriers. Recently, advances in devices that permit flow control in 3-dimensional (3D) channels [7–10] and accommodate multiplexed assays in a small area have been reported [11–14]. Flow control, however, requires precision fabrication of fluidic channels using materials that can support a variety of liquids. A number of paper patterning methods have been reported, including photolithography [1, 15], etching [16], inkjet printing [17, 18], wax printing [19, 20], embossing [21], vapor phase deposition [22], flexography printing [23], screen-printing [24, 25], stamping [26–28], and photopolymerization [29]. Advantages and disadvantages of these patterning methods have been well documented in recently published review articles [2–6].

Wax printing is the most common technique since paper can be easily patterned and rapidly produced in mass quantities using this method. While wax printing has many advantages, it has several drawbacks, including leakage when used with organic solvents and surfactant-containing solutions. As a result, applications requiring non-aqueous and/or surfactant-containing solutions have been limited. Moreover, the penetration of wax into paper is normally achieved by heating, but the isotropic wax spreading during heating leads to asymmetric boundaries on the front and back sides of paper, which limites patterns to be produced in high resolutions [19, 20]. Generating fine features is especially important for achieving multiplexed, high-density μPADs and for precisely controlling flow because the geometry of patterns plays an important role in determining the flow behavior. Photolithography provides an alternative fabrication method that can achieve high spatial resolution [1, 15]. However, photolithography is limited by its cost and complexity, as well as background signals generated from the use of photoresist. Photopolymerization can also provide high resolution features [29] but frequently suffers from contamination during the soaking and development processes. Therefore, a new fabrication method capable of producing impermeable barriers with high resolution and compatibility with various solutions is still needed.

Patterning paper is frequently accomplished by either filling the pores of the cellulose fibers with a hydrophobic barrier material or by chemically modifying the fiber surface with hydrophobic materials. Common hydrophobic agents include photoresist [1, 15], solid wax [18–20, 25–27], polystyrene [17, 23–25], poly(dimethylsiloxane) [28], fluoropolymer [14], photopolymer [29] and hydrophobic silanes [16, 21, 30]. Recently a fabrication procedure

using everyday school glue was reported that was resistant to organic solvents and surfactant-containing solutions [31]. Parafilm®, as a low-cost, sticky, stretchable material used extensively in laboratories around the world for sealing or protecting vessels, has also been used to fabricate μPADs [32–34]. Parafilm® consists mainly of paraffin wax, has a melting temperature of ~60°C, and is resistant to many chemical substances such as alcoholic compounds, saline solutions, inorganic acids, and alkaline solutions [33]. Previous μPADs made with Parafilm® have been generated either by using a mask-guided infilling of a sheet of Parafilm® [32] or by direct infilling of photolithographically patterned [33] or craft-cut [34] Parafilm® into porous paper using a heated press. These patterning methods provide a simple and inexpensive way to fabricate 2D or 3D μPADs. However, the former method cannot produce separated channels with well-defined dimensions because each channel needs an independent shadow mask. The latter approaches also provide limited spatial resolution due to the lateral spreading of paraffin wax together with the inward moving during the heated press.

Other than using hydrophobic materials, cutting the paper to make boundaries is another simple and attractive patterning method in μPAD fabrication. Historically, cutting was used as a standard method to fabricate simple paper devices for dipstick and lateral flow assays [3]. More complicated μPADs have been generated using both craft-cutters [35] and laser cutting/engraving machines [36]. When a laser cutting is used, the process is rapid, automated, highly reproducible, and compatible with high-throughput production [6, 37]. Despite these advantages, the laser cutting/engraving method can create closed-loop barriers without reducing the mechanical integrity of the system, which is nearly impossible with other cutting equipment.

Here, we present two methods that combine Parafilm® and laser cutting to generate μPADs that address current gaps in the field. Fig. 1 shows a schematic of the fabrication approaches. The first step of the fabrication involved hot pressing Parafilm® and paper together to create a fused structure. Based on the degree of fusion, two types of paper were created: laminated paper (*l*-paper) resulting from partial fusion and infused paper (*i*-paper) resulting from full fusion of the two layers. *l*-paper was patterned using a CO_2 laser engraver with optimized settings to selectively remove the paper but not the Parafilm®, which is similar to the process used for patterning nitrocellulose on polyester backing [38]. Subsequently a desired shape of Parafilm® would be exposed to become a hydrophobic barrier for defining active fluidic within the hydrophilic sample area in paper. Since the uncut paper remained strongly bonded to the Parafilm®, precisely shaped closed-loop patterns that are hard to make with wax printing were achievable via ablative etching. The ablation method could create barriers as narrow as 137 ± 22 μm. As a proof of concept, a miniaturized paper 384-zone plate four times smaller than the size of standard 96-well plates (128 × 86 mm^2) was fabricated with *l*-paper. Patterning *i*-paper required first fully cutting out desired shapes in both *i*-paper and unmodified paper. The two pieces were then fitted together using a method that resembled a jigsaw puzzle-like strategy and bonded with a heated press. Under heat, the paraffin reflowed from the *i*-paper into the unmodified paper creating a permanent bond. Using free-standing sheets of jigsaw-patterned *i*-paper, two relatively complex 3D μPADs (a push-on valve and a time-gated fluid distributor) were fabricated to highlight the advantages of *i*-paper relative to traditional fabrication methods.

2. Experimental

2.1. Materials and chemicals

Dimethylformamide (DMF), sodium dodecyl sulfate (SDS), hexadecyltrimethylammonium bromide (CTAB), and Coomassie Brilliant Blue R-250 dye were purchased from Sigma-Aldrich (St. Louis, MO). Acetonitrile was purchased from Yakuri Pure Chemicals (Japan) and methanol was obtained from Daejung Chemicals & Metals (South Korea). Whatman chromatography paper (grade 1, porosity ≅ 0.67), Whatman filter paper (grade 4, porosity ≅ 0.70) and Parafilm® M (Pechiney Plastic Packaging Company) were purchased from VWR international (Bridgeport, NJ). Fluoropolymer-coated release liner (Scotchpak™ 9744, 3M) was acquired from 3M (St. Paul, MN). Food dye solutions (Food Colors, Kroger), transparency film (Highland 901) and clear packing tape (Scotch, 3M) were purchased from a local stationary store.

2.2. Preparation of the laminated and infused substrates

The *l*-paper was prepared by thermally bonding chromatography paper and Parafilm®. The bonding process was performed on glass at 45°C and 0.10 MPa using a hot press (Model 4122, Carver) for 3 min. To avoid surface contamination, the top surface of the paper was covered with a transparency film. *i*-paper was produced by pressing at higher temperature and pressure to fully fuse the paper and the paraffin. Pieces of filter paper and Parafilm® were aligned and sandwiched between fluoropolymer-coated liners for easy separation after pressing. To optimize the fabrication conditions for both types of materials, the permeation behavior of Parafilm® into paper was investigated at different combinations of temperature (35 – 65°C) and pressure (0 – 6 MPa) over a period of 10 min. The thicknesses and contact angles of the pressed samples were measured by a micrometer (#895, Pittsburgh) and a drop shape analyzer (DSA30A, Krüss), respectively. The cross-sectional structures were observed by an optical microscope equipped with a digital camera (AM-423, Dino-Eye).

2.3. Patterning in the laminated and infused substrates

Patterns of hydrophilic cellulose paper in *l*-paper and *i*-paper were constructed using a benchtop CO_2 laser (30 W Zing 24, Epilog Laser) from drawings prepared with Corel Draw X4 software. To generate channels in *l*-paper, the upper paper layer was selectively ablated as the focused laser spot scanned over the sample surface. The ablation process was carried out using raster mode for broad ablation of a selected region and followed by vector mode to create a sharp channel boundary. For the jigsaw patterning, an *i*-paper and a native paper were cut using higher power laser irradiation in vector mode. The detailed laser operation conditions are summarized in Supplementary Table 1. The cut-out spaces in *i*-paper were replaced by pieces of paper with the same shape and thickness as the *i*-paper. The paper parts were intentionally prepared to be ~0.15 mm smaller than the openings in *i*-paper for easy insertion into the hollow area. After fitting the paper pieces into the corresponding openings in *i*-paper, all components were bonded together on a laboratory hotplate with a 1 kg weight at 75°C, causing the paraffin wax to diffuse into the edges of the unmodified paper. The fabricated structures were inspected by microscopy, and dye solutions were used to observe wetting and flow behavior.

3. Results and Discussion

3.1. Permeation behavior of Parafilm® into porous paper

The ability of Parafilm® to infuse Whatman filter paper was studied first by measuring the resulting thickness of a structure as a function of heat and pressure over a period of 10 min (Fig. 2A). The bottom dashed line corresponds to a pressure-dependent thickness change of paper as a reference. As expected, the paper thicknesses varied by only 2 μm over the temperature range studied (35 – 65°C). In contrast, the bilayer of paper and Parafilm® became thinner as the pressure and/or temperature increased. A cross-sectional microscopy image of a sample fabricated at mild conditions (55°C and 0.76 MPa) on a base transparency film is shown in Fig. 2B, clearly displaying the bilayer structure. An aqueous solution of green dye was used to visualize the paper. A grey intermediate layer is distinct at the interface between paper and Parafilm®, suggesting a partial fusion. When the bilayer was pressed at 65°C and 6.1 MPa, the material became non-wetting (Fig. 2C) with a contact angle of 112 ± 3° which is similar to that of Parafilm® (108 ± 5°). The wetting effect indicates the presence of Parafilm® on the surface. The slightly higher contact angle on *i*-paper comparing to that on Parafilm® was attributed to different surface roughness of *i*-paper and Parafilm®. Rougher surfaces are known to have a higher contact angle for identical materials [39]. The average thickness of *i*-paper was 150 μm, which is slightly less than that of native paper. The resulting *i*-paper has asymmetric surfaces: one side has a rough composite surface, while the opposite side has a smooth surface coated by a thin film of remaining Parafilm®. Upon optimization, 65°C and 6.1 MPa was chosen for *i*-paper fabrication to ensure complete fusion of paper with paraffin.

The hot-pressing process simply employed a hotplate and a heavy load. The *l*-paper was successfully prepared by pressing the bilayer stack (area = 6.45 cm^2) with a 1 kg metal disk on a 75°C hotplate. The *i*-paper could be produced under even less controlled conditions with an increased weight and/or temperature. This method provides a simple and low-cost approach for achieving equivalent products to those made with specialized hot-press machines.

3.2. Patterning resolutions in *l*-paper and *i*-paper

μPAD performance depends on the ability to make high resolution channels defined by impermeable barriers. The minimum barrier and channel dimensions possible for *i*-paper and *l*-paper μPADs were investigated using three different device designs. In Fig. 3A, a blue dye solution was perfectly confined within the inner circle of concentric ring patterns in *l*-paper when the ablated boundary line width was set beyond 125 μm. The average barrier width measured by microscopy was 137 ± 22 μm along the horizontal direction (left and right sides) and 182 ± 15 μm along the vertical direction (upper and lower sides) for 20 measurements, implying that the minimum barrier width was 137 ± 22 μm when using a 125 μm line width. The direction-dependent width change resulted from an elliptical laser beam shape. When the line width was set at 100 μm, the solution spread to the outer circle in two out of five test zones. The average barrier width at left and right positions was found to be 65 ± 26 μm. The smallest barrier width produced here is smaller than that produced by other patterning methods including photolithography [15], screen printing [24], wax printing [19],

inkjet printing [17], stamping [28] and photopolymerization [29]. The only comparable methods for patterning critical barrier widths are deep UV-lithography patterning of silane-modified paper at 137 ± 21 μm [16] and direct-write photopolymerization patterning of nitrocellulose membrane at ~60 μm [29]. Compared to these methods, the ablation process is inherently simpler and does not expose the paper to solvents or chemicals that may interfere with any following assay. Consequently, the ablation technique is highly efficient in producing arrays of small patterns with complex shapes in *I*-paper.

We next tested the ability to generate narrow channels in *I*-paper using the ablative etching. Paper channel widths were designed to gradually increase upward from 200 to 1000 μm as shown in Fig. 3B. Well-defined channels were created when channels when widths were >250 μm. The actual channel width was reduced by approximately 150 μm from the nominal values due to the expansion of the thermally-induced ablation region along the boundary lines (Fig. S1). As a result, a very narrow paper channel (~100 μm) could be achieved in *I*-paper. It is worth mentioning that the flow rate along the narrow channel depends strongly on width. No flow was observed in the 100 μm channel (a nominal value of 250 μm), while the observed flow rates steadily increased with channel width in the range of 150 – 850 μm. The slow flow rate in small channels is likely caused by a limited number of connected capillaries in the fiber network at this channel size and/or fast evaporation of water due to the high surface area to volume of the resulting structures. While there is significant interest in generating fast/slow flows to reduce/increase assay time, the ability that this fabrication method offers to modulate flow rate based on channel dimensions is advantageous.

Finally, the patterning resolutions in *i*-paper based devices were tested. To precisely fit a cut paper piece to a cut-out hollow area in *i*-paper, the actual dimensions of *i*-paper and native paper were compared after being cut to the designed feature size. Since the cutting process removed unintended area during line cutting due to the width of the laser spot, the average width of the hollow strip in *i*-paper was ~180 μm larger than the designed value, while the paper channel width decreased by ~140 μm (Fig. S2). Fig. 3C shows a free-standing μPAD fabricated using *i*-paper with nominal channel widths from 100 to 1500 μm. The gap between paper and *i*-paper was observed to be partially filled with paraffin as a result of the lateral permeation during the hot press. Since the paper channel width was prepared with a margin of 150 μm for easy insertion into the *i*-paper, the narrowest channel that could be fabricated was 130 μm. Flow of a green dye solution was realized in all channel widths. As with the channels formed in *I*-paper, flow rates decreased as a function of channel width. The flow rates were comparable to those obtained in suspended native paper.

Chemical compatibility of the channels formed in *I*-paper was tested using aqueous surfactant (SDS or CTAB) solutions and common organic solvents such as acetonitrile, methanol and DMF. In Fig. 3D, the ablated hollow barriers with a width of 200–500 μm retained all test solutions within circular detection zones. As a comparison purpose, wax-printed barriers were also tested for the same solutions. However, the patterned wax boundary could not function as an impermeable barrier as shown in Fig. 3D. The ability to confine a variety of solutions provides the potential for *I*-paper μPADs to be used with analyses requiring non-aqueous solutions and bioassays requiring surfactant solutions. Existing μPADs, with a few exceptions[31], are typically challenged by these types of

solutions, making the *l*-paper approach very attractive for complex chemical and biochemical analyses.

3.3. μPADs fabricated using *l*-paper or *i*-paper

3.3.1. A miniaturized paper 384-zone plate—As the first demonstration of μPADs made using *l*-paper, a paper multi-zone plate was fabricated as displayed in Fig. 4. The miniaturized paper 384-zone plate was chosen to highlight the high-resolution feature of the ablation method for making μPADs. The horizontal and vertical lengths of the paper plate are a factor of two smaller than standard 96- and 384-well microtiter plates (128 mm × 86 mm). The paper plate consisted of an array of 16 by 24 zones, each having a circular shape (diameter = 1.86 mm) with a center-to-center distance of 2.25 mm. The ablated 150 μm barriers worked well throughout the whole testing zones. The demonstration proves that multiple spot tests are possible in the detection zones with a small amount of dye solution (50–100 nL). Consequently, this miniaturized paper multi-zone plate provides many opportunities in high-throughput tests for various chemical analyses and bioassays, since the hollow barrier was confirmed to block the flow of a wide range of liquids including organic solvents and surfactant solutions.

3.3.2. Manual push-on valve—As a second illustration, a manual push-on valve reported previously by Martinez et al. [37] was chosen to demonstrate the applicability of stacking and bonding layers of patterned *i*-paper without any additional adhesive layers. The bonding was easily performed by pressing the aligned layers on a 75 °C hotplate for 5 min. Fig. 5A displays a cross-sectional schematic of the paper valve consisting of three *i*-paper layers, while Fig. S3A shows photographs of the individual layers before the bonding. Operation of the 3D paper valve is shown in Movie S1 with snapshots shown in Fig. 5B. A spontaneous flow of solution through the paper channel started when the push point was activated. The previous 3D valve device required 7 layers of paper and tape for fabrication [37]. However, our device required only three layers of patterned *i*-paper and had a 100% success rate in operation. The layer reduction was attributed to the mechanical properties of the *i*-paper as well as the ability to bond layers without additional materials. Fewer-layered devices are essentially less laborious and cheaper to make with possibly lower systematic errors across different batches.

3.3.3. Time-gated fluid distributor—Lastly, a 3D μPAD capable of distributing a single sample fluid into four outlets with different arrival times was achieved by bonding multiple layers of patterned *i*-paper. Fig. 6A shows a schematic structure of the time-gated fluid distributor consisting of five layers with individual layers prior to assembly shown in Fig. S3B. Fig. 6B and 6C display pictures taken at the front and back sides, respectively. Operation of the μPAD fluid distributor is shown in Movie S2 as follows: 1) 50 μL of water is dropped on the inlet hole of the 1st layer; 2) the sample is split into four paper channels in the 2nd layer; 3) each flow passes through the wax-patterned time delay channels in the 3rd layer where each channel has a different design that controls flow rate; and 4) the resultant water dissolves pre-deposited dye in paper pads of the 4th layer and then moves to paper circles of the 5th layer. The time delay channels in the 3rd layer are four circular copy paper pieces with different wax-printed grid structures: the same line-to-line distance of 0.7 mm

and different line thicknesses of 0, 0.1, 0.3, and 0.5 mm (a photograph of the grids is shown in Fig. S3B) using the knowledge gained from prior studies of flow as a function of line width. The average arrival times obtained from 4 devices were 27 ± 15 s with no grid pattern (red), 43 ± 8 s for the narrow wax line (green), 55 ± 10 s for the medium wax line (yellow), and 69 ± 11 s for the wide wax line (blue) as displayed in Fig. 6C. the large standard deviation associated with the no grid pattern is likely the result of variations in fluid contact between paper layers. As with the valve structures, a 100% fabrication success rate for 5-layered 3D μPADs was achieved. These results demonstrate that the flow arrival time could be regulated simply by changing a wax line width in grid pattern.

4. Conclusion

Here, we have reported two new methods of forming hydrophilic and hydrophobic patterns for the fabrication of μPADs. The methods utilize the properties of the Parafilm® (thermoplastic and chemical inertness) combined with precision machining using a desktop commercial CO_2 laser via either ablative etching or through-cutting. The first method was based on the selective ablation of a paper partially fused with Parafilm® to create *I*-paper, while the second method created an open space in *i*-paper using a cutting process followed by re-bonding of unmodified paper into the opening. The patterning methods provided high resolution with the ability to prepare channels ≤150 μm in width and were demonstrated to be compatible with various chemicals including organic solvents and surfactants that cannot be used with traditional wax barriers. Utility of the simple one-step ablation method was demonstrated in the fabrication of a miniaturized paper 384-zone plate with a size of 64 × 43 mm^2. Using the simple thermal bonding of patterned *i*-paper layers, we successfully fabricated two 3D μPADs, a manual push-on valve, and a time-gated fluid distributor. While examples of these devices exist in literature, the new methods reported here provide higher resolution and more reliable fabrication and operation owing to the characteristics of the combined structures made from Parafilm® and porous paper.

Supplementary Material

Refer to Web version on PubMed Central for supplementary material.

Acknowledgments

This research was supported by Basic Science Research Program through the National Research Foundation of Korea (NRF) funded by the Ministry of Education, Science and Technology (NRF-NRF-2016R1D1A1A02937490). This work was also supported in part by the National Institutes of Health through the Institute for Environmental Health and Science (ES023496).

References

1. Martinez AW, Phillips ST, Butte MJ, Whitesides GM. Patterned Paper as a Platform for Inexpensive, Low-Volume, Portable Bioassays. Angewandte Chemie International Edition. 2007; 46:1318–20. [PubMed: 17211899]
2. Martinez AW, Phillips ST, Whitesides GM, Carrilho E. Diagnostics for the Developing World: Microfluidic Paper-Based Analytical Devices. Anal Chem. 2010; 82:3–10. [PubMed: 20000334]
3. Yetisen AK, Akram MS, Lowe CR. Paper-based microfluidic point-of-care diagnostic devices. Lab on a Chip. 2013; 13:2210–51. [PubMed: 23652632]

4. Cate DM, Adkins JA, Mettakoonpitak J, Henry CS. Recent Developments in Paper-Based Microfluidic Devices. Anal Chem. 2015; 87:19–41. [PubMed: 25375292]
5. Jiang X, Fan ZH. Fabrication and Operation of Paper-Based Analytical Devices. Annual Review of Analytical Chemistry. 2016; 9:203–22.
6. Yang Y, Noviana E, Nguyen MP, Geiss BJ, Dandy DS, Henry CS. Paper-Based Microfluidic Devices: Emerging Themes and Applications. Anal Chem. 2017; 89:71–91. [PubMed: 27936612]
7. Martinez AW, Phillips ST, Whitesides GM. Three-dimensional microfluidic devices fabricated in layered paper and tape. Proceedings of the National Academy of Sciences. 2008; 105:19606–11.
8. Liu H, Crooks RM. Three-Dimensional Paper Microfluidic Devices Assembled Using the Principles of Origami. Journal of the American Chemical Society. 2011; 133:17564–6. [PubMed: 22004329]
9. Lewis GG, DiTucci MJ, Baker MS, Phillips ST. High throughput method for prototyping three-dimensional, paper-based microfluidic devices. Lab on a Chip. 2012; 12:2630–3. [PubMed: 22706568]
10. Schilling KM, Jauregui D, Martinez AW. Paper and toner three-dimensional fluidic devices: programming fluid flow to improve point-of-care diagnostics. Lab on a Chip. 2013; 13:628–31. [PubMed: 23282766]
11. Carrilho E, Phillips ST, Vella SJ, Martinez AW, Whitesides GM. Paper Microzone Plates. Anal Chem. 2009; 81:5990–8. [PubMed: 19572563]
12. Liu H, Li X, Crooks RM. Paper-Based SlipPAD for High-Throughput Chemical Sensing. Anal Chem. 2013; 85:4263–7. [PubMed: 23586896]
13. Chinnasamy T, Segerink LI, Nystrand M, Gantelius J, Andersson Svahn H. Point-of-Care Vertical Flow Allergen Microarray Assay: Proof of Concept. Clinical Chemistry. 2014; 60:1209–16. [PubMed: 25006224]
14. Deiss F, Matochko WL, Govindasamy N, Lin EY, Derda R. Flow-Through Synthesis on Teflon-Patterned Paper To Produce Peptide Arrays for Cell-Based Assays. Angewandte Chemie International Edition. 2014; 53:6374–7. [PubMed: 24729420]
15. Martinez AW, Phillips ST, Wiley BJ, Gupta M, Whitesides GM. FLASH: A rapid method for prototyping paper-based microfluidic devices. Lab on a Chip. 2008; 8:2146–50. [PubMed: 19023478]
16. He Q, Ma C, Hu X, Chen H. Method for Fabrication of Paper-Based Microfluidic Devices by Alkylsilane Self-Assembling and UV/O3-Patterning. Anal Chem. 2013; 85:1327–31. [PubMed: 23244032]
17. Abe K, Suzuki K, Citterio D. Inkjet-Printed Microfluidic Multianalyte Chemical Sensing Paper. Anal Chem. 2008; 80:6928–34. [PubMed: 18698798]
18. Li, Za, Hou, L., Zhang, W., Zhu, L. Preparation of paper micro-fluidic devices used in bio-assay based on drop-on-demand wax droplet generation. Analytical Methods. 2014; 6:878–85.
19. Carrilho E, Martinez AW, Whitesides GM. Understanding Wax Printing: A Simple Micropatterning Process for Paper-Based Microfluidics. Anal Chem. 2009; 81:7091–5. [PubMed: 20337388]
20. Lu Y, Shi W, Jiang L, Qin J, Lin B. Rapid prototyping of paper-based microfluidics with wax for low-cost, portable bioassay. ELECTROPHORESIS. 2009; 30:1497–500. [PubMed: 19340829]
21. Cai L, Wang Y, Wu Y, Xu C, Zhong M, Lai H, et al. Fabrication of a microfluidic paper-based analytical device by silanization of filter cellulose using a paper mask for glucose assay. Analyst. 2014; 139:4593–8. [PubMed: 25045759]
22. Kwong P, Gupta M. Vapor Phase Deposition of Functional Polymers onto Paper-Based Microfluidic Devices for Advanced Unit Operations. Anal Chem. 2012; 84:10129–35. [PubMed: 23113699]
23. Olkkonen J, Lehtinen K, Erho T. Flexographically Printed Fluidic Structures in Paper. Anal Chem. 2010; 82:10246–50. [PubMed: 21090744]
24. Sameenoi Y, Nongkai PN, Nouanthavong S, Henry CS, Nacapricha D. Onestep polymer screen-printing for microfluidic paper-based analytical device ([small mu]PAD) fabrication. Analyst. 2014; 139:6580–8. [PubMed: 25360590]

25. Dungchai W, Chailapakul O, Henry CS. A low-cost, simple, and rapid fabrication method for paper-based microfluidics using wax screen-printing. Analyst. 2011; 136:77–82. [PubMed: 20871884]
26. de Tarso Garcia P, Garcia Cardoso TM, Garcia CD, Carrilho E, Tomazelli Coltro WK. A handheld stamping process to fabricate microfluidic paper-based analytical devices with chemically modified surface for clinical assays. RSC Advances. 2014; 4:37637–44.
27. Zhang Y, Zhou C, Nie J, Le S, Qin Q, Liu F, et al. Equipment-Free Quantitative Measurement for Microfluidic Paper-Based Analytical Devices Fabricated Using the Principles of Movable-Type Printing. Anal Chem. 2014; 86:2005–12. [PubMed: 24444190]
28. Dornelas KL, Dossi N, Piccin E. A simple method for patterning poly(dimethylsiloxane) barriers in paper using contact-printing with low-cost rubber stamps. Analytica Chimica Acta. 2015; 858:82–90. [PubMed: 25597806]
29. He PJW, Katis IN, Eason RW, Sones CL. Laser-based patterning for fluidic devices in nitrocellulose. Biomicrofluidics. 2015; 9:026503. [PubMed: 26015836]
30. Glavan AC, Martinez RV, Maxwell EJ, Subramaniam AB, Nunes RMD, Soh S, et al. Rapid fabrication of pressure-driven open-channel microfluidic devices in omniphobic RF paper. Lab on a Chip. 2013; 13:2922–30. [PubMed: 23719764]
31. Cardoso TMG, de Souza FR, Garcia PT, Rabelo D, Henry CS, Coltro WKT. Versatile fabrication of paper-based microfluidic devices with high chemical resistance using scholar glue and magnetic masks. Analytica Chimica Acta. 2017; 974:63–8. [PubMed: 28535882]
32. [accessed May 23, 2017] http://blogs.rsc.org/chipsandtips/2012/04/10/simple-and-rapid-fabrication-of-paper-microfluidic-devices-utilizing-parafilm
33. Yu L, Shi ZZ. Microfluidic paper-based analytical devices fabricated by low-cost photolithography and embossing of Parafilm[registered sign]. Lab on a Chip. 2015; 15:1642–5. [PubMed: 25710591]
34. Koesdjojo MT, Pengpumkiat S, Wu Y, Boonloed A, Huynh D, Remcho TP, et al. Cost Effective Paper-Based Colorimetric Microfluidic Devices and Mobile Phone Camera Readers for the Classroom. Journal of Chemical Education. 2015; 92:737–41.
35. Fenton EM, Mascarenas MR, López GP, Sibbett SS. Multiplex Lateral-Flow Test Strips Fabricated by Two-Dimensional Shaping. ACS Applied Materials & Interfaces. 2009; 1:124–9. [PubMed: 20355763]
36. Nie J, Liang Y, Zhang Y, Le S, Li D, Zhang S. One-step patterning of hollow microstructures in paper by laser cutting to create microfluidic analytical devices. Analyst. 2013; 138:671–6. [PubMed: 23183392]
37. Fu E, Lutz B, Kauffman P, Yager P. Controlled reagent transport in disposable 2D paper networks. Lab on a Chip. 2010; 10:918–20. [PubMed: 20300678]
38. Spicar-Mihalic P, Toley B, Houghtaling J, Liang T, Yager P, Fu E. CO 2 laser cutting and ablative etching for the fabrication of paper-based devices. Journal of Micromechanics and Microengineering. 2013; 23:067003.
39. Quéré D. Wetting and Roughness. Annual Review of Materials Research. 2008; 38:71–99.

Biographies

Yuanyuan Yang is a postdoctoral fellow at Colorado State University under the supervision of Dr. Charles Henry. She received her Ph.D. in Analytical Chemistry under the supervision of Dr. Parastoo Hashemi at Wayne State University in 2016. Her research focuses on the development of electrochemical and colorimetric paper-based analytical devices to detect biological and environmental hazards.

Yong Shin Kim received a PhD in chemistry from Korea Advanced Institute of Science and Technology (KAIST) in 1997. After his degree, he worked as a senior research member at Electronics and Telecommunications Research Institute (ETRI) in South Korea for

developing flat panel display devices and miniaturized electronic nose systems. Since 2007, he has been employed at Hanyang University in South Korea as a professor. Now his research activities are focused on the development of chemical sensors and paper-based fluidic devices by the aid of novel concept, new fabrication techniques, and smart nanomaterials.

Charles Henry is a Professor of Chemistry, Chemical & Biological Engineering, and Biomedical Engineering as well as Chair of Chemistry at Colorado State University. He received his Ph.D. in Analytical Chemistry under the supervision of Dr. Ingrid Fritsch at the University of Arkansas, and was an NIH postdoctoral fellow at the University of Kansas under the supervision of Dr. Susan Lunte. His research interests lie broadly in the areas of microfluidics and electrochemistry with application to questions in bioanalytical and environmental chemistry.

Highlights

- New Parafilm-based method for fabricating paper-based microfluidic devices is described.
- Small, well-defined channels and structures can be created using common fabrication tools
- Resulting structures can support flow in organic and surfactant-containing solutions which cannot be achieved with wax printed materials
- Examples of a small 384-well microtiter plate and two valving systems are demonstrated.

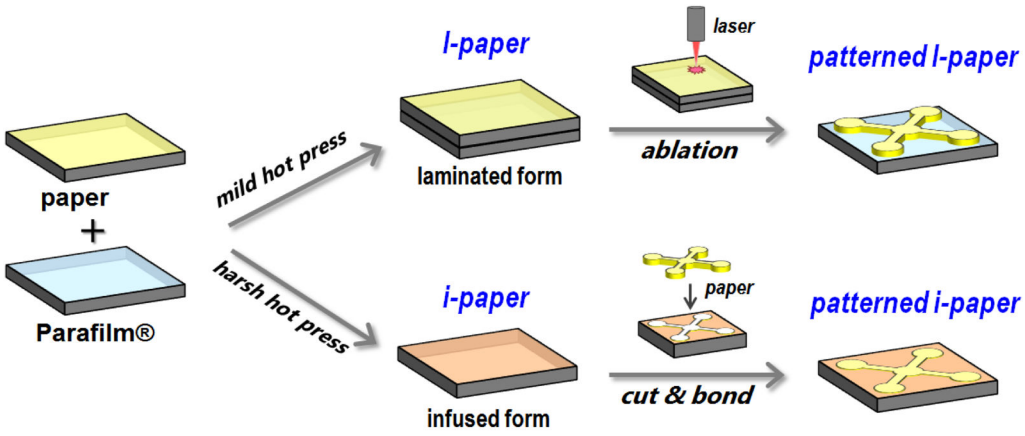

Fig. 1.

Schematic of the approaches to prepare two different types of Parafilm paper and channels for flow control. In the upper half of the figure, the *l*-paper was patterned via ablation by scanning a laser spot over the paper surface. In the lower half of the figure, a paper cut-out was inserted into a hollow area in *i*-paper cut to an identical shape with the laser cutter, and then bonded at the boundary, similar to the principle of a jigsaw puzzle.

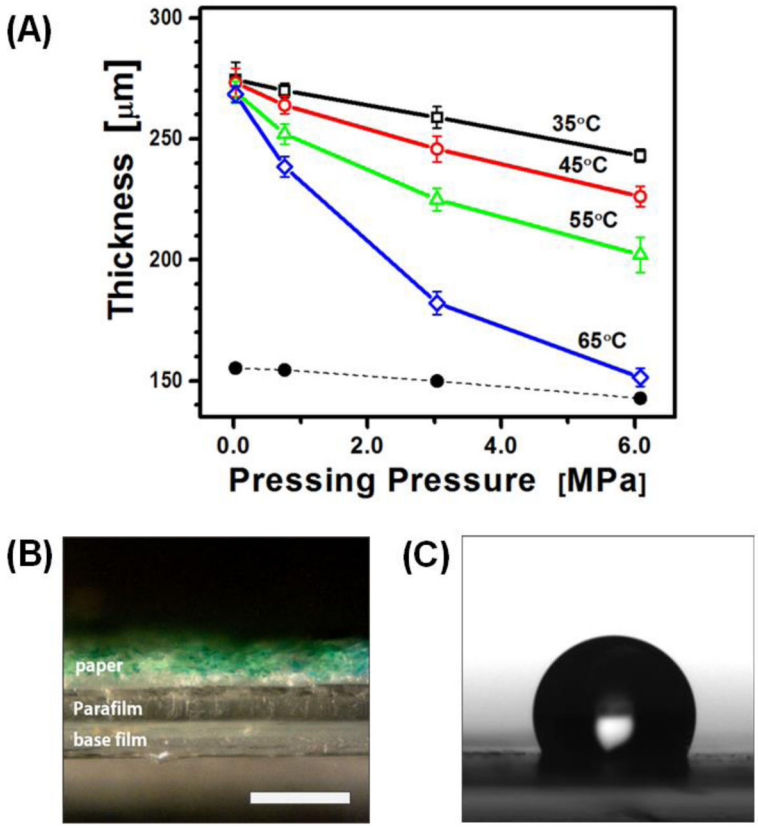

Fig. 2.

(A) Thickness variation of bilayers of paper and Parafilm® pressed at different temperatures and pressures. The bottom solid circles indicate an average thickness of a single piece of paper over the different temperatures. (B) Cross-sectional image of the laminated sample pressed at 55°C and 0.76 MPa. The length of the scale bar is 250 μm. (C) Side view of 2 μL water drop on a paper side of the infused sample prepared at 65°C and 6.1 MPa.

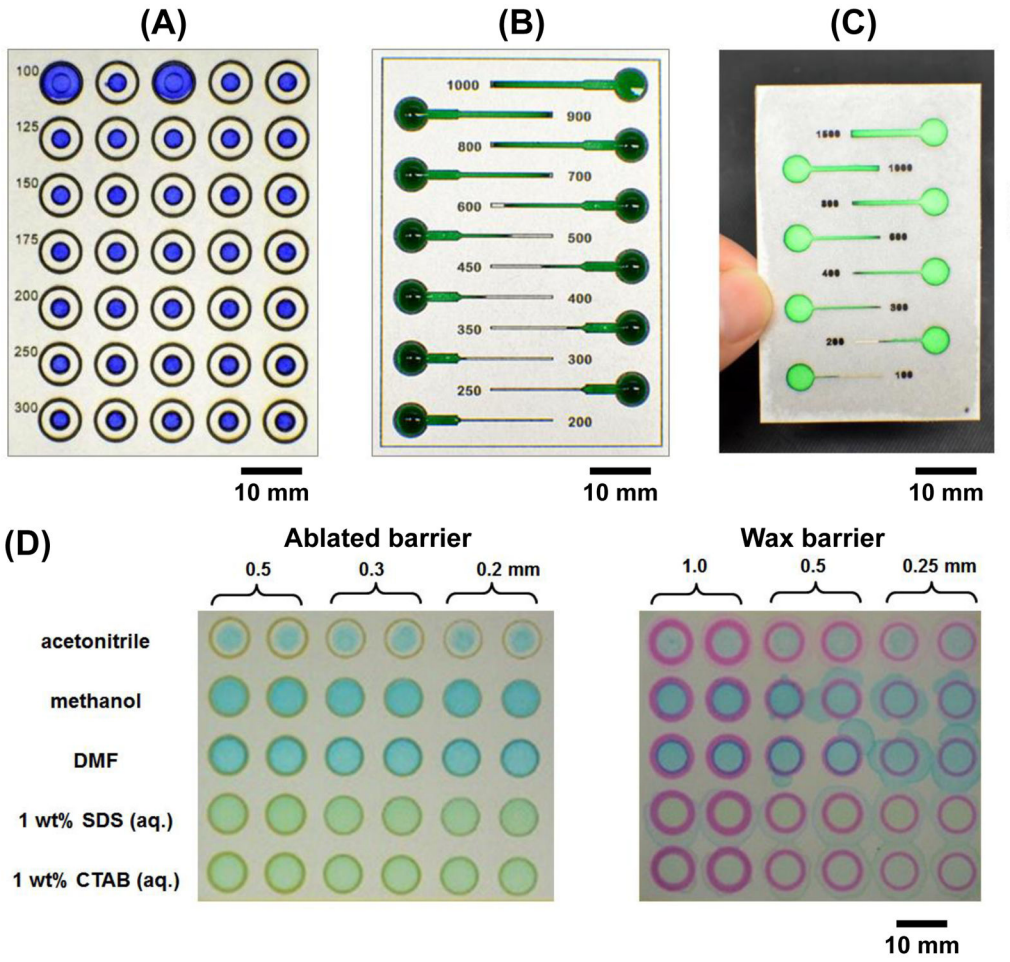

Fig. 3.

(A) A photograph of a 35-zone test plate patterned by the ablation in *I*-paper for evaluating the smallest fluidic barrier. The ablated barrier regions are shown in black. Each detection zone has two concentric rings where the inner ring (ϕ = 3 mm) acts as a test barrier for a 2 μL blue dye solution. The set barrier width was increased from 100 to 300 μm as indicated in a left side of the image. Pictures of tested devices fabricated by (B) the ablation in *I*-paper and (C) the jigsaw method in *i*-paper for evaluating a minimum channel width. A 10 μL green dye solution was manually dispensed at the circular inlet pads. The fluid was advanced to a test strip channel whose nominal width (μm) is displayed nearby the channel tip. (D) Pictures showing chemical compatibilities of the ablated (left) and wax-printed (right) barriers with three organic solvents (acetonitrile, methanol and DMF) and two surfactant aqueous solutions (SDS and CTAB). The top values display a barrier width used for defining detection zones in drawings. Small amount of dye was added into the solutions for a visual purpose.

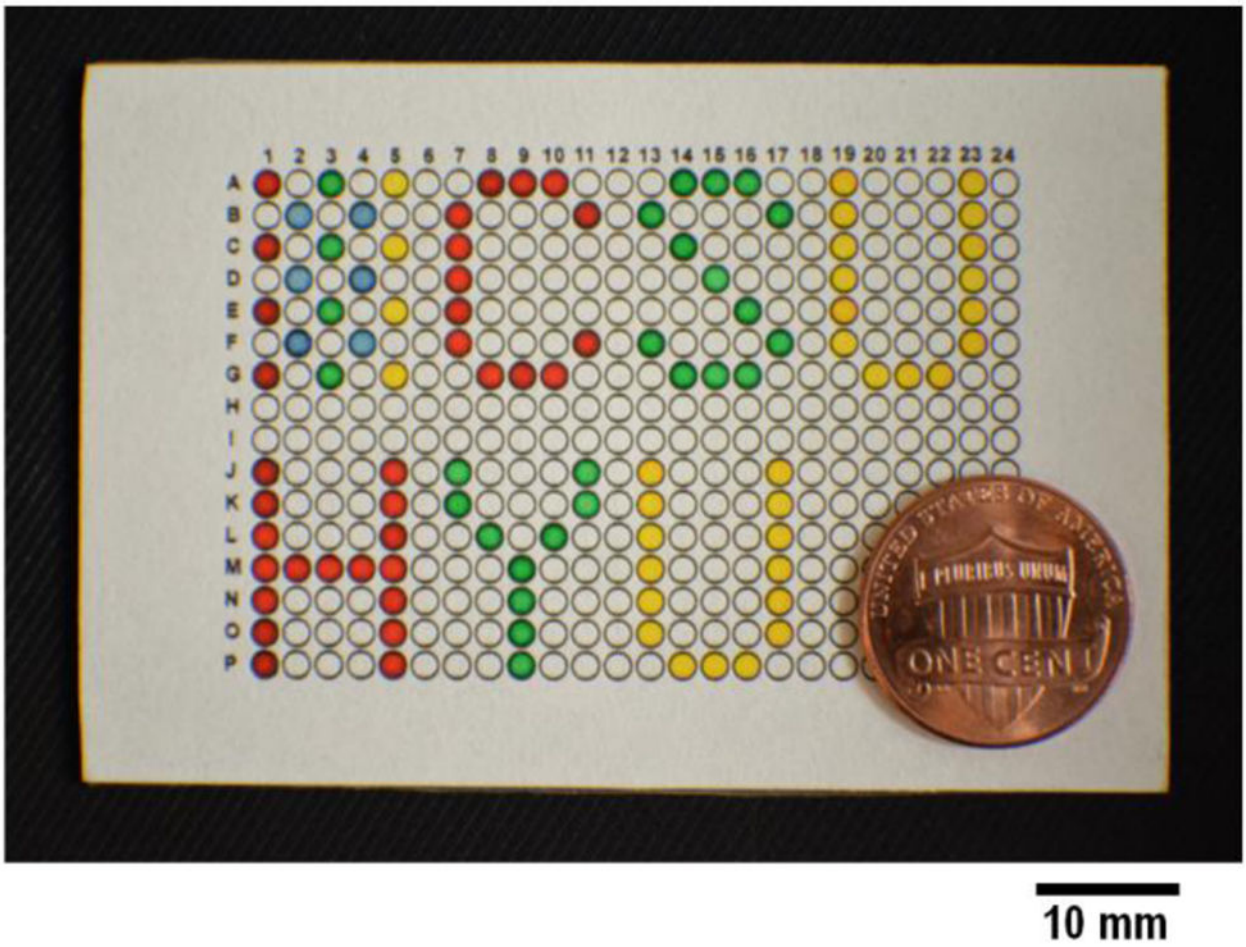

Fig. 4.

A picture of a paper 386-zone plate produced by the ablation patterning of *I*-paper. Four dye solutions with different colors were manually dispensed on specific zones using a micropipette. The diameter of each detection zone and its center-to-center distance were 1.86 mm and 2.25 mm, respectively.

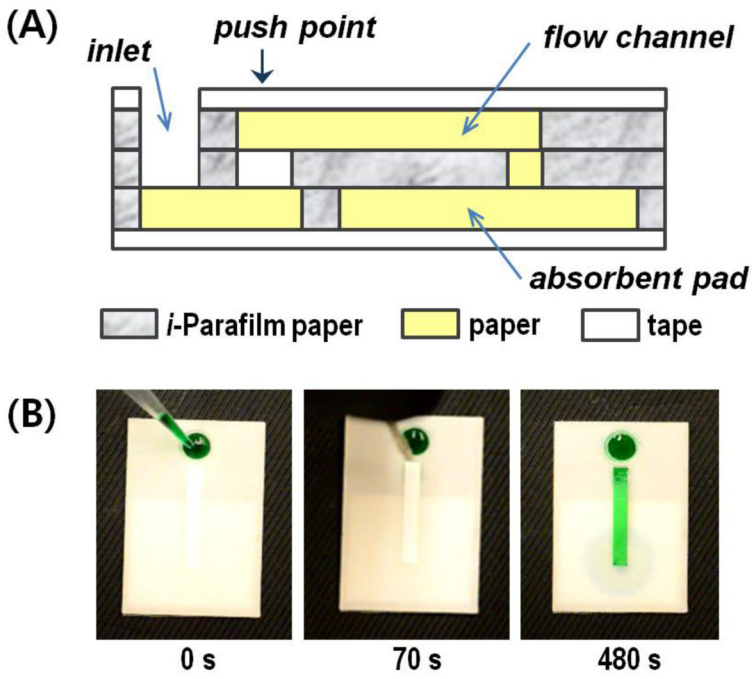

Fig. 5.

(A) Schematic of a cross-sectional μPAD structure of the fabricated push-on valve. (B) Snapshots showing an operation of the paper valve. The push point was pressed with a small metal tip at 70 s after adding 10 μL of green dye solution to the inlet. The top and bottom layers were enclosed by clear tapes.

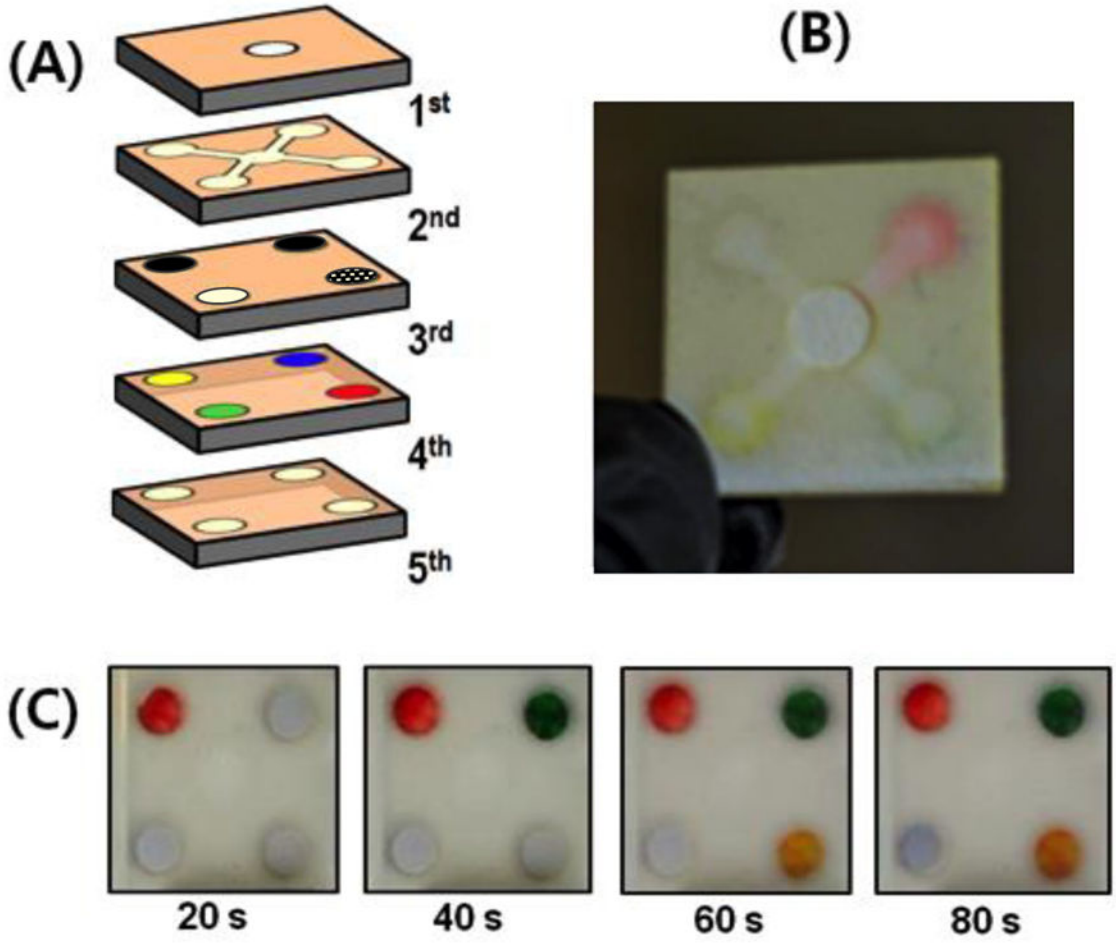

Fig. 6.

(A) A schematic of the expanded 5-layer structure of the time-gated fluid distributor. (B) A front image of the free-standing fluid distributor. (C) Snapshots of the back side taken at different times after supplying a 50 μL aqueous solution into the front center inlet.